

# Photothermal Spectroscopy (PTS) of PMMA thin layer using micro-ring resonators (MRRs)



**GIOVANNA RICCHIUTI**

*TUW (Vienna, Austria) - Munster Technological University (Cork, Ireland)*

**Giovanna Ricchiuti<sup>1,2,3</sup>, Jesús Hernán Mendoza-Castro<sup>4,1</sup>, Anton Walsh<sup>2,3</sup>, Artem S. Vorobev<sup>4,2,3</sup>, Simone Iadanza<sup>5</sup>, Marco Grande<sup>4</sup>, Bernhard Lendl<sup>1\*</sup> and Liam O'Faolain<sup>2,3\*</sup>**

1. Institute of Chemical Technologies and Analytics, TU Wien, Getreidemarkt 9/164-UPA, 1060, Vienna, Austria

2. Centre for Advanced Photonics and Process Analysis, Munster Technological University, T12 T66T Bishopstown, Cork, Ireland

3. Tyndall National Institute, T12 PX46 Cork, Ireland

4. Department of Electrical and Information Engineering, Polytechnic University of Bari, 4, 70126 Bari, Italy

5. Laboratory of Quantum and Nanotechnologies Paul-Scherrer-Institut ODRA/114 Forschungsstrasse 111 - 5232 Villigen PSI Schweiz

[WWW.OPTAPHI.EU](http://WWW.OPTAPHI.EU)

4 SEPTEMBER 2023

C-PASS 2023

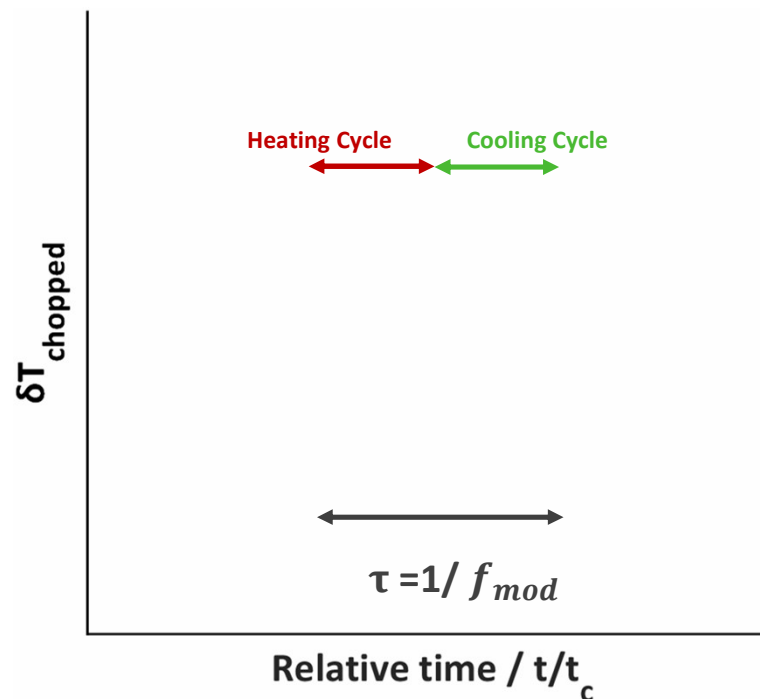


OPTAPHI has received funding from the European Union's Horizon 2020 research and innovation programme under the Marie Skłodowska-Curie grant agreement No. 860808



# Photothermal Spectroscopy principle

- Mid-IR spectroscopy  
 $\nu = 4000 - 400 \text{ cm}^{-1}$   
 $\lambda = 2.5 - 25 \mu\text{m}$
- Quantitative and qualitative information of molecular species
- Label-free & non-destructive



## PHOTOTHERMAL SPECTROSCOPY

Temperature and refractive index (Photothermal)

$$\text{Signal} \propto \Delta T = \frac{P(\tilde{\nu}) \alpha(\tilde{\nu}) d}{\rho C_p V f_{mod}}$$

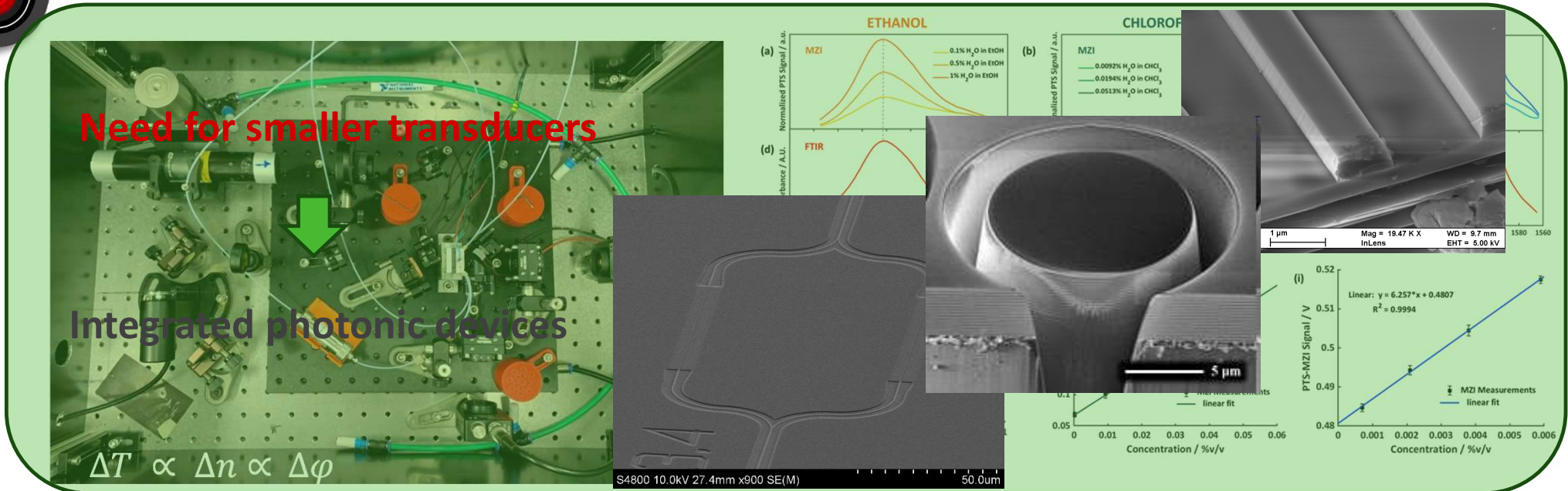
$$\Delta T \propto \Delta n$$

**P ... Optical power**

A ... Beam cross section area  
 $\alpha(\tilde{\nu})$ .....Absorption coefficient  
d.....Optical pathlength  
 $f_{mod}$  ... Modulation Frequency  
 $c_p$  ... Heat Capacity  
 $\rho$  ... Density  
V..... Volume



# Free-space Photothermal Spectroscopy Mach-Zehnder Interferometer (PTS-MZI)<sup>2</sup>



PTS enables for sensor miniaturization<sup>1</sup>:  $\text{Signal} \propto \Delta T = \frac{P(\tilde{\nu}) \alpha(\tilde{\nu}) d}{\rho C_P V f_{mod}}$

- Decrease test sample volume and of reagents/solvents/waste
- Shorten the duration of the analysis
- Different conditions of heat transfer
- Smaller optical pathlengths **d**

1. Bialkowski, S.E. Photothermal Spectroscopy Methods for Chemical Analysis; John Wiley & Sons, 1996.  
2. Ricchiuti, G.; Dabrowska, A.; Pinto, D.; Ramer, G.; Lendl, B. Dual-Beam Photothermal Spectroscopy Employing a Mach-Zehnder Interferometer and an External Cavity Quantum Cascade Laser for Detection of Water Traces in Organic Solvents. *Anal. Chem.* 2022, 94 (47), 16353–16360. <https://doi.org/10.1021/acs.analchem.2c03303>.

Slide 2

C-PASS 2023

20 December 2023

WWW.OPTAPHI.EU

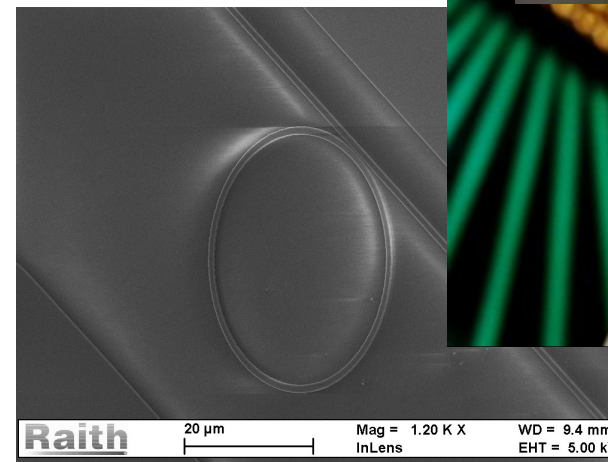
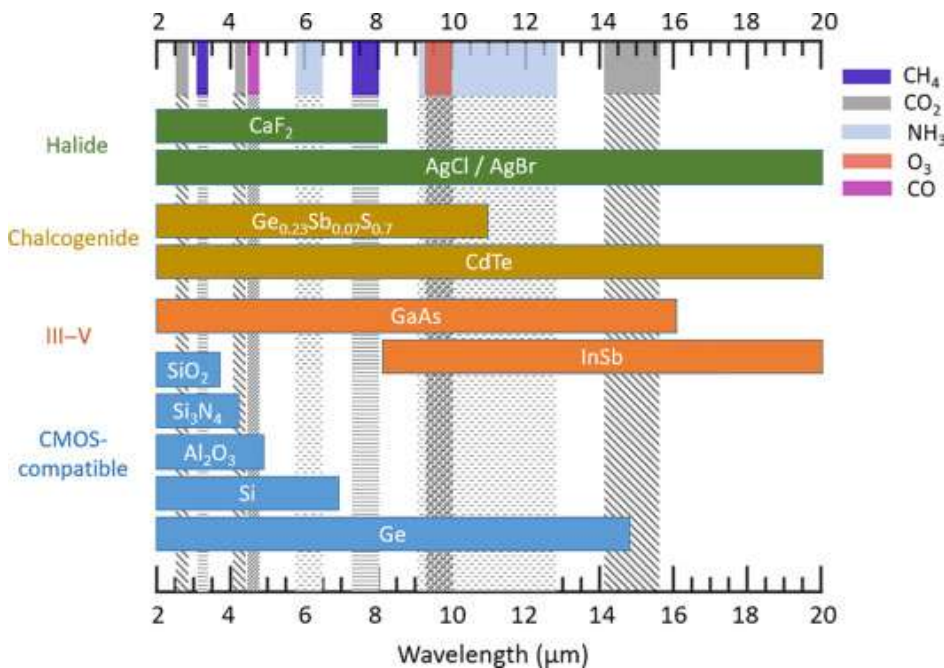
# Photonic Integrated Circuits (PICs)

Integrated circuit are widely used for:

- Data communications
- Sensing
- Industrial applications
- Biomedical applications

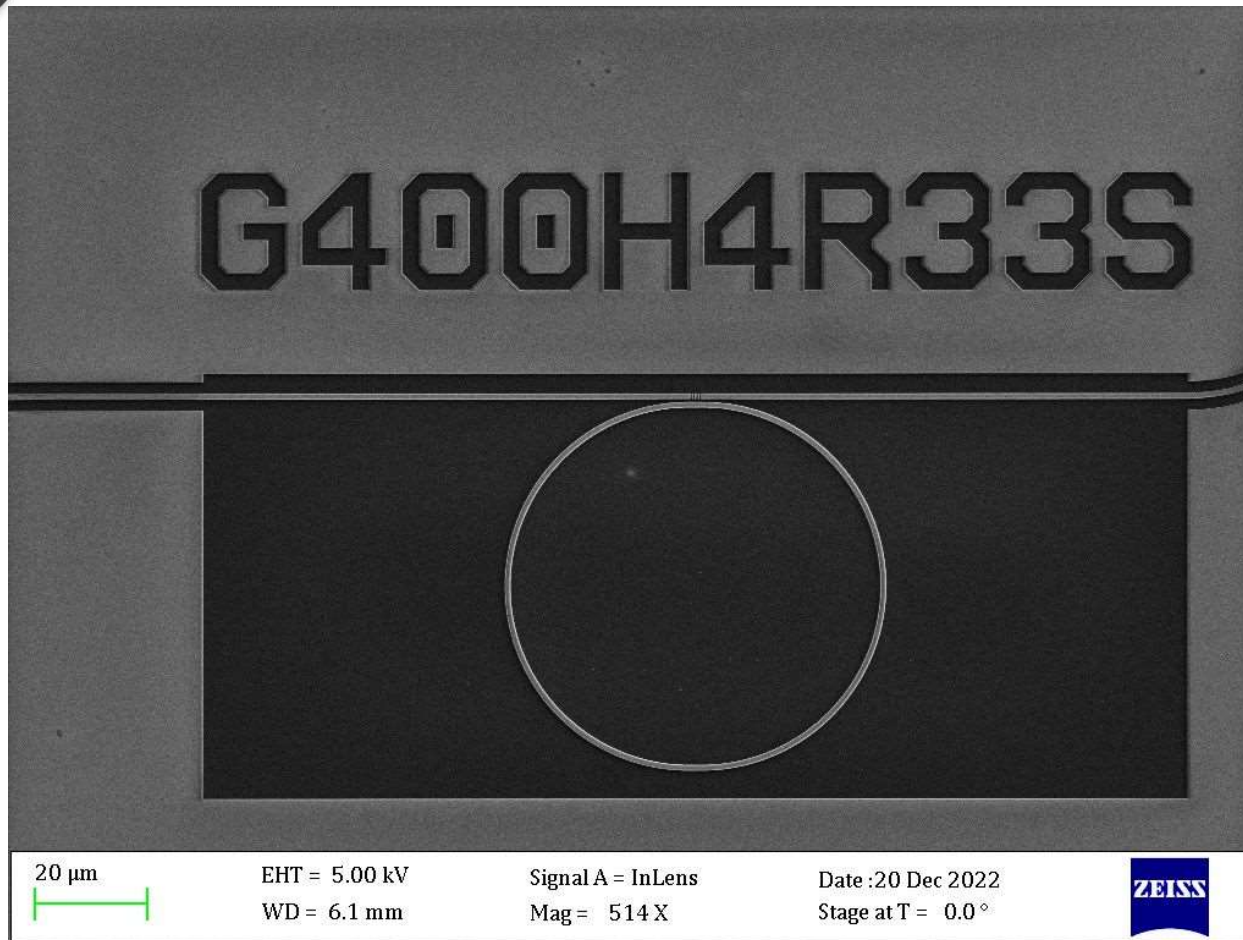
Main features:

- Low cost
- Compact and light
- Low power consumption
- High efficiency
- High speed
- Low thermal issues
- Large integration capacity



C-PASS 2023

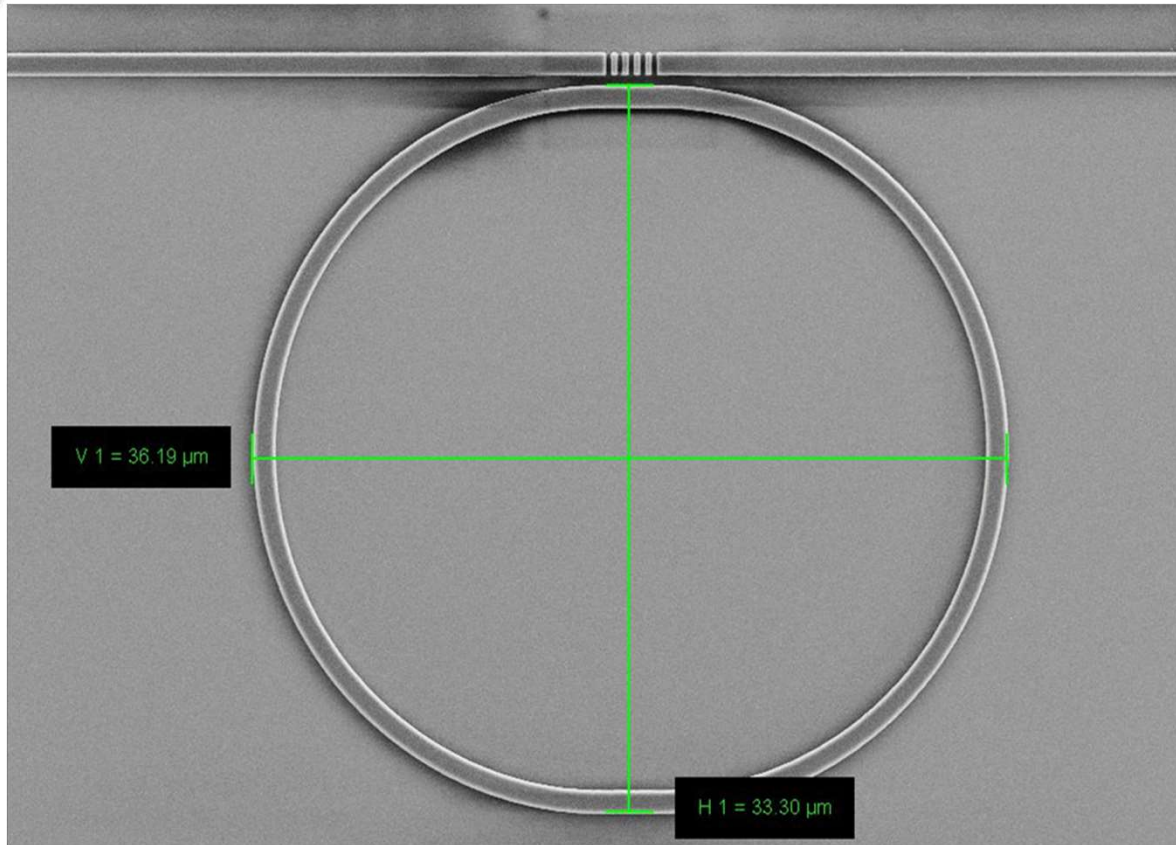
# The sensitive device: micro-ring resonators (MRRs)



The sensitive device is a MRR made in  $\text{Si}_3\text{N}_4$  ( $n \sim 2$ )



# The sensitive device: micro-ring resonators (MRRs)

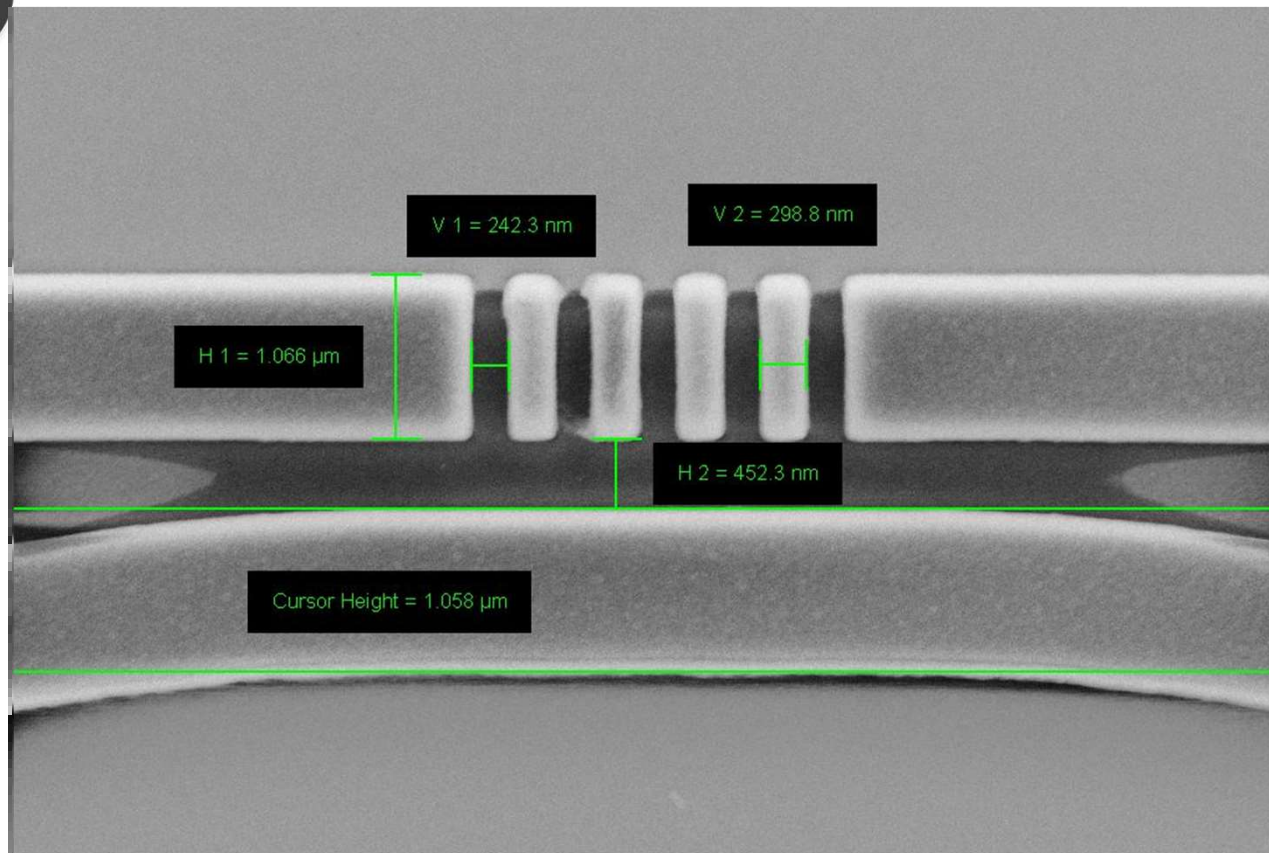


The sensitive device is a MRR made in  $\text{Si}_3\text{N}_4$  ( $n \sim 2$ )

The used rings have a radius of 16 or  $33 \mu\text{m}$



# The sensitive device: micro-ring resonators (MRRs)



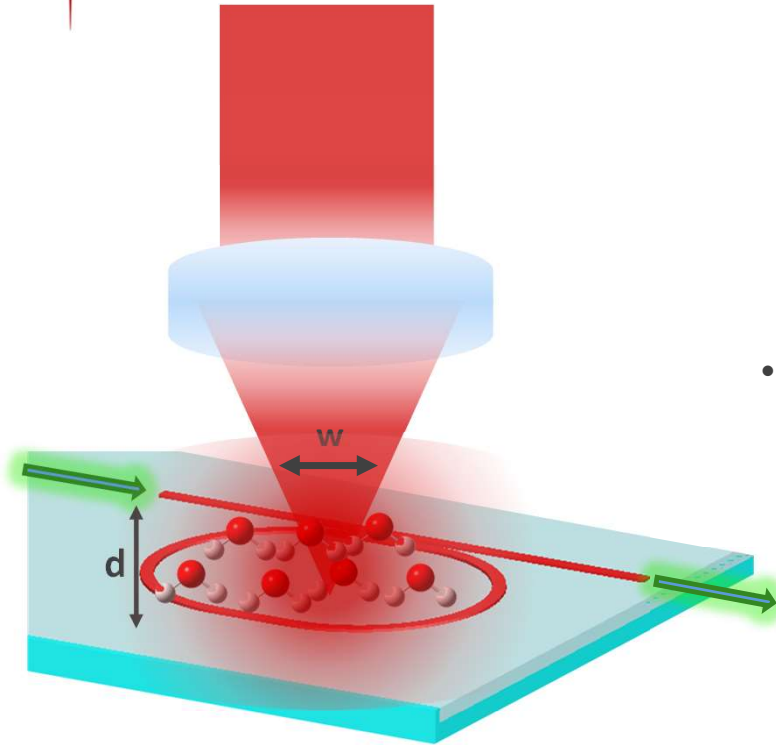
The sensitive device is a MRR made in  $\text{Si}_3\text{N}_4$  ( $n \sim 2$ )

The used rings have a radius of 16 or 33 μm

MRR partially transmitting elements (PTE) in the gap region have been engineered to achieve high Q-factor and sharp asymmetric Fano resonances



# The sensitive device: micro-ring resonators (MRRs)



- $n_{eff}$  change due to the change of  $n_{clad}$  in the waveguide

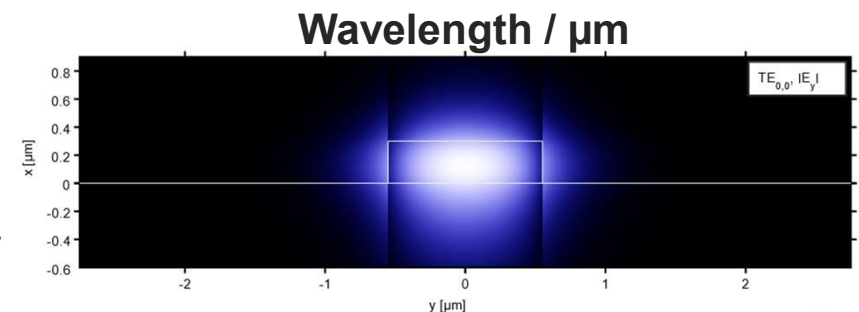
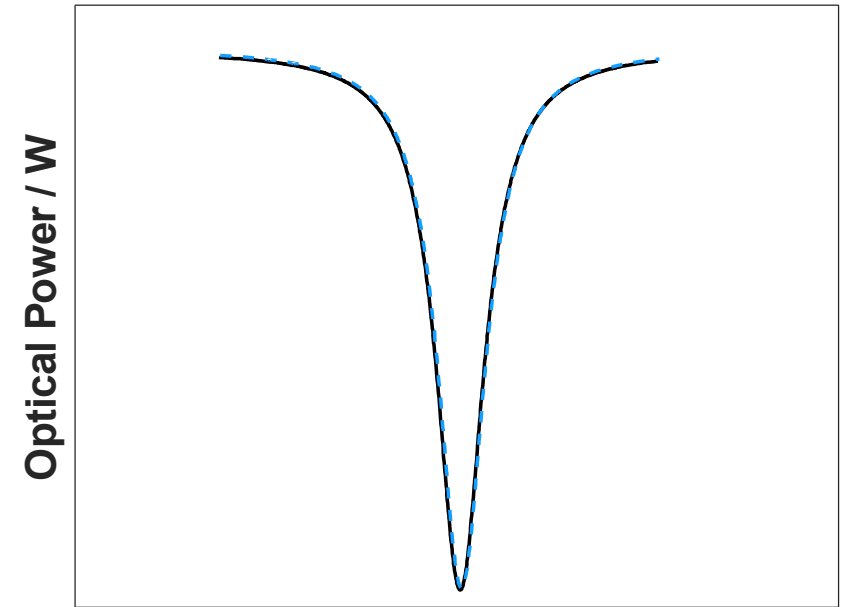


$$\Delta\lambda_{Res} \propto \Delta n_{eff}$$

- $T$  change photoinduced by an excitation source, introduce a  $n_{eff}$  change related to the  $\frac{dn}{dT}$  of the materials



$$\Delta\lambda_{Res} \propto \Delta T \propto \Delta n_{eff}$$

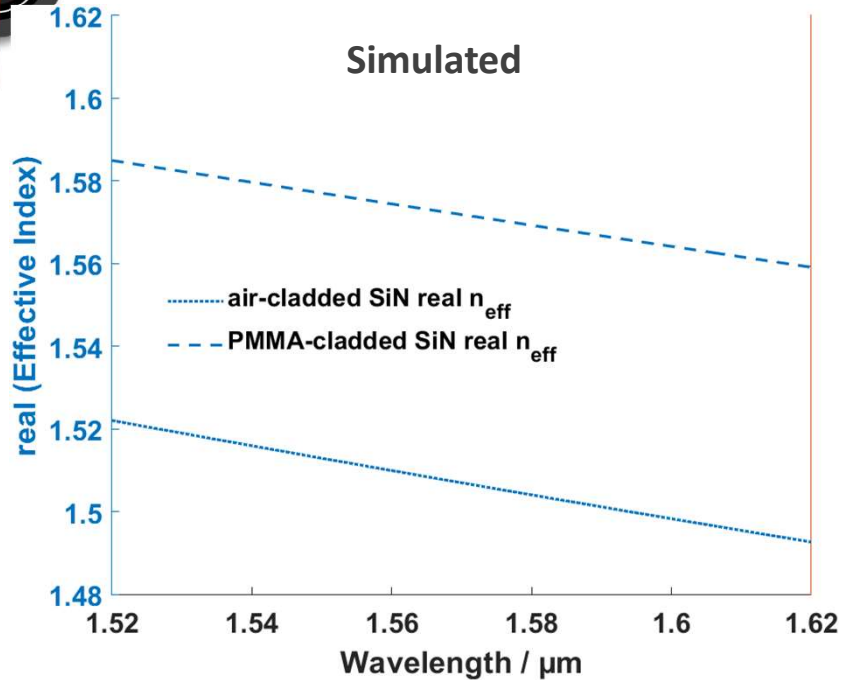


**Refractive index and Temperature sensor**

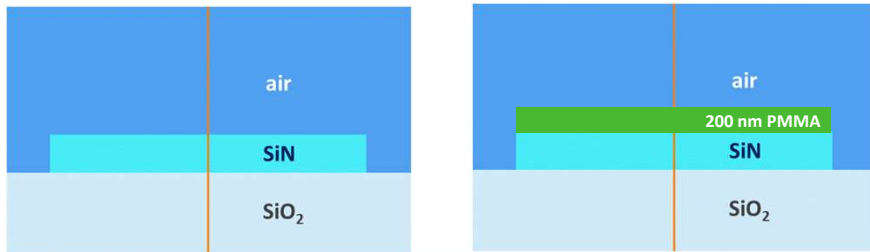
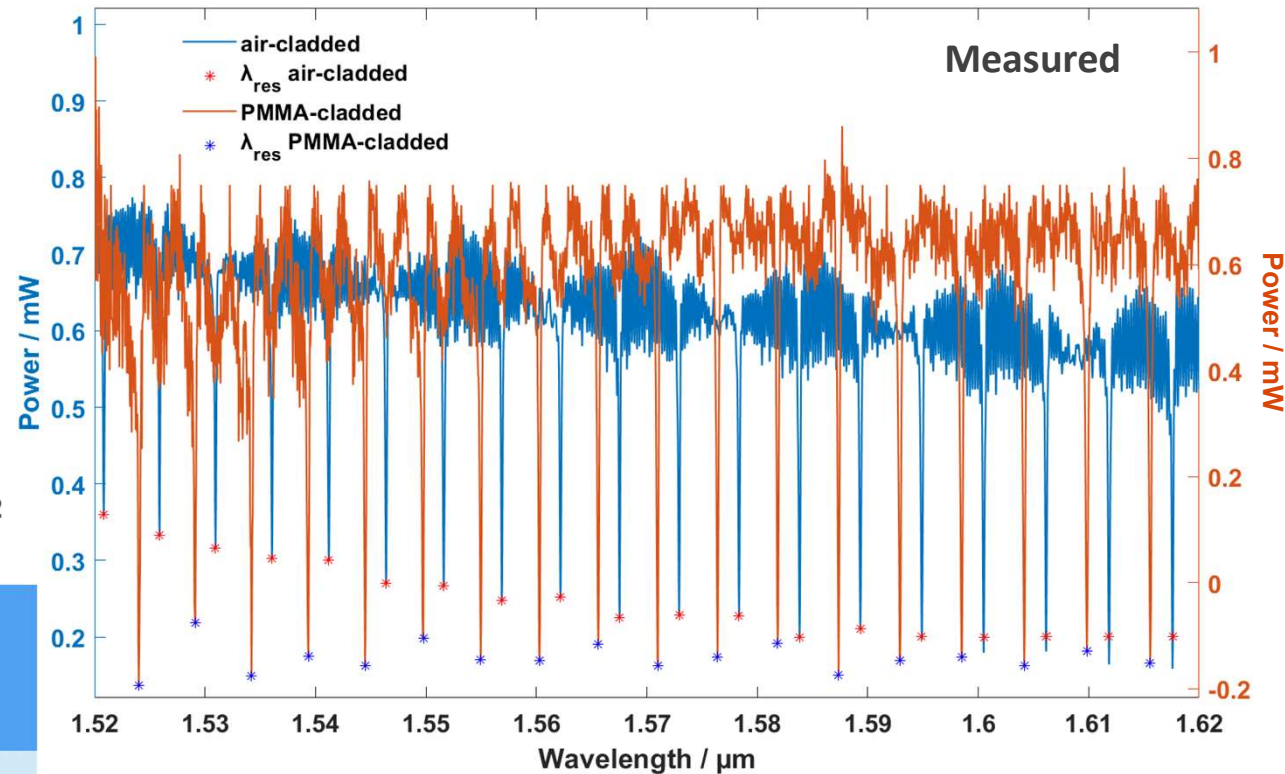




# The analyte: Polymethylmethacrylate (PMMA), $n_{\text{clad}}$



**Ring: G400H4R33S T holder: 20°C**



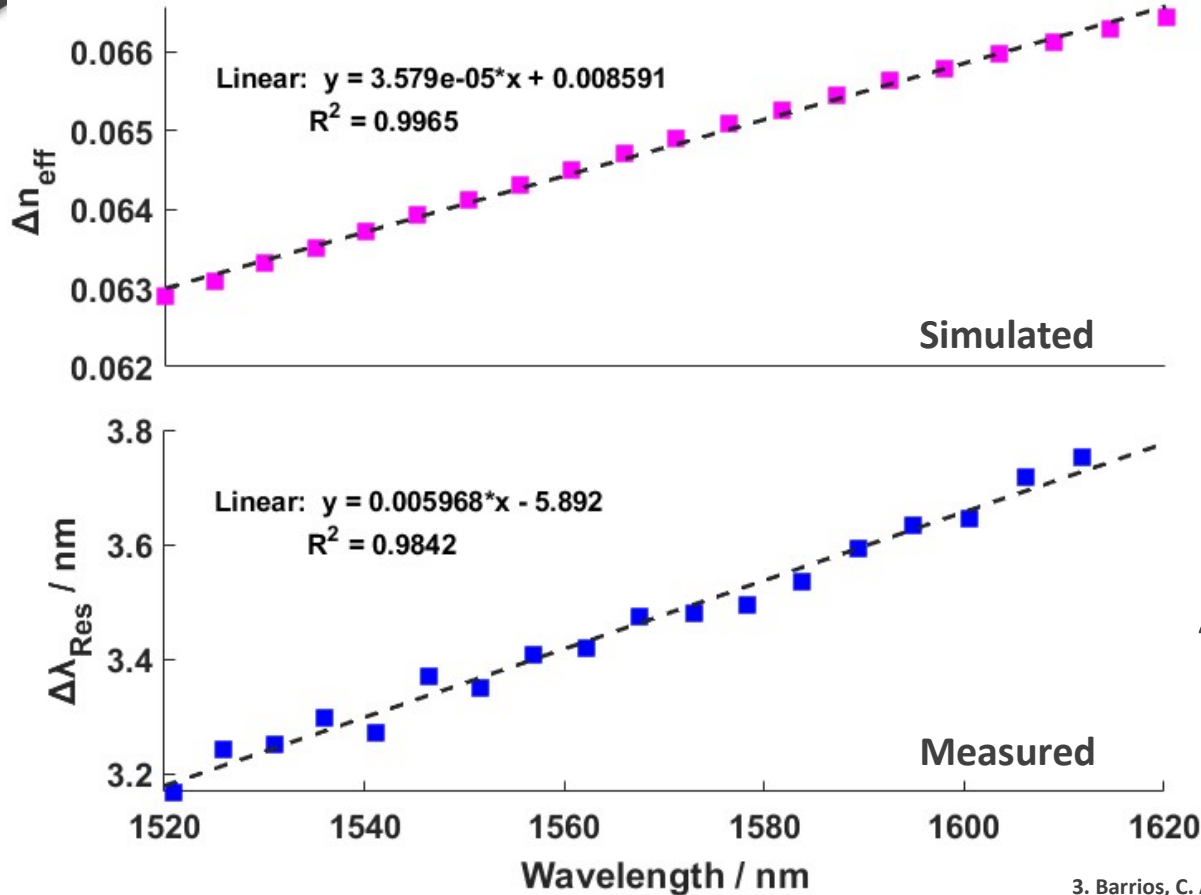
C-PASS 2023

20 December 2023

WWW.OPTAPHI.EU



# The analyte: Polymethylmethacrylate (PMMA), $n_{clad}$



$$\Delta n_{clad} (@1550 \text{ nm}) \sim 0.48 \text{ RIU}$$



$$\Delta n_{eff} \sim 0.064$$



$$\Delta \lambda_{Res} \sim \boxed{3.35 \text{ nm}} + m \cdot FSR$$

Calculated<sup>3</sup>

$$\Delta \lambda_{Res} = -\Delta n_{eff} \frac{2\pi}{\lambda_{Res,0}} \cdot \left( \frac{2\pi n_g(\lambda_{Res,0})}{\lambda_{Res,0}^2} \right)^{-1}$$

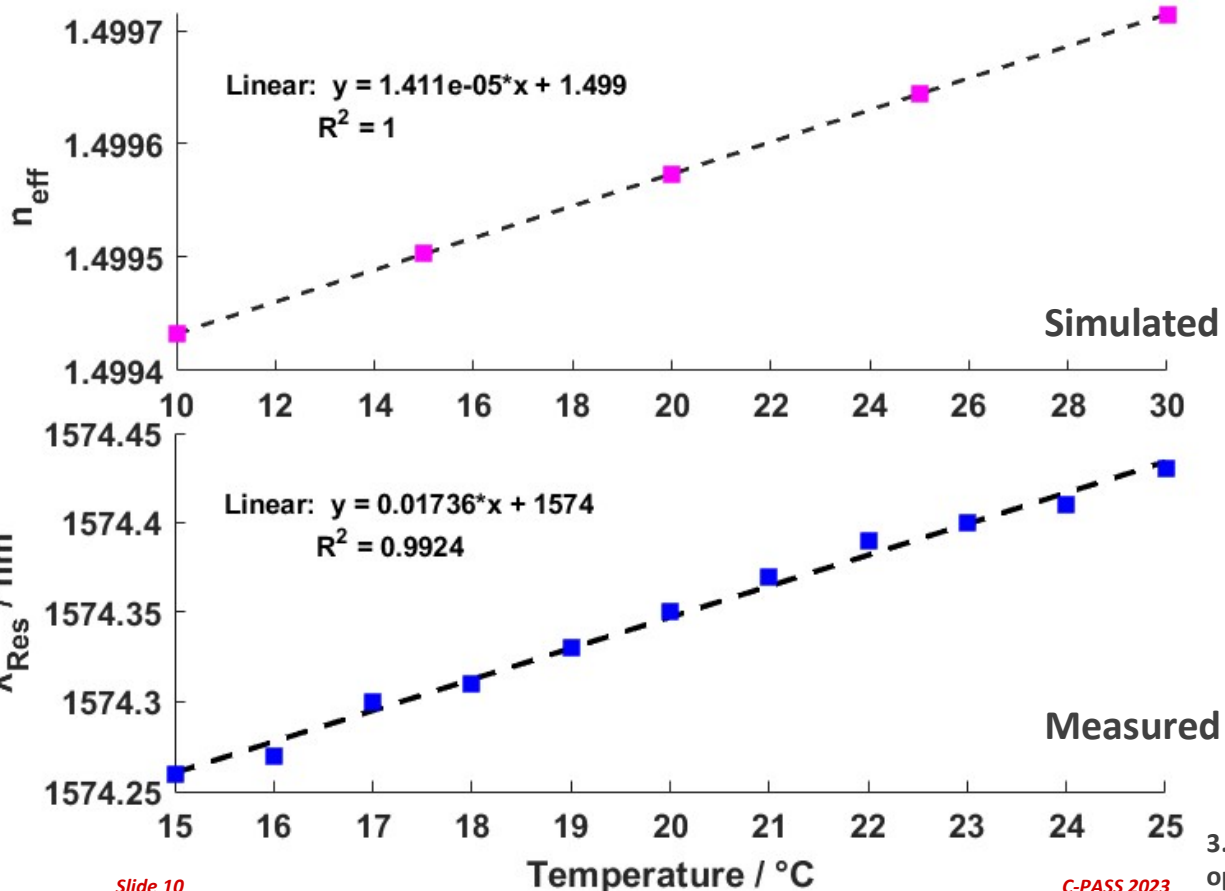
$$\Delta \lambda_{Res} = \boxed{3.1 \text{ nm}}$$

Slide 9

3. Barrios, C. A. Optical Slot-Waveguide Based Biochemical Sensors. Sensors 2009, 9 (6), 4751–4765. <https://doi.org/10.3390/s90604751>, 20 December 2023



# The thermo-optical effect of SiN, $dn/dT$



**SiN TOC =  $2.1e-5$  [RIU/°C]**

$\Delta T_{SiN} \sim + 1^\circ C$

$\frac{\Delta n_{eff}}{\Delta T} \sim 1.411e-5$

$\frac{\Delta \lambda_{Res}}{\Delta T} \sim 17 \text{ pm}$

Calculated<sup>3</sup>

$\frac{\Delta \lambda_{Res}}{\Delta T} = \left( \frac{\Delta n_{eff}}{\Delta T} + n_{eff} \alpha_{TH} \right) \cdot \frac{\lambda_{Res}}{n_{eff}}$

$\frac{\Delta \lambda_{Res}}{\Delta T} = 18 \text{ pm}$

3. Rabus, D. G. Integrated Ring Resonators: The Compendium; Springer series in optical sciences; Springer: Berlin Heidelberg, 2007

Slide 10

C-PASS 2023

20 December 2023



# The experimental setup

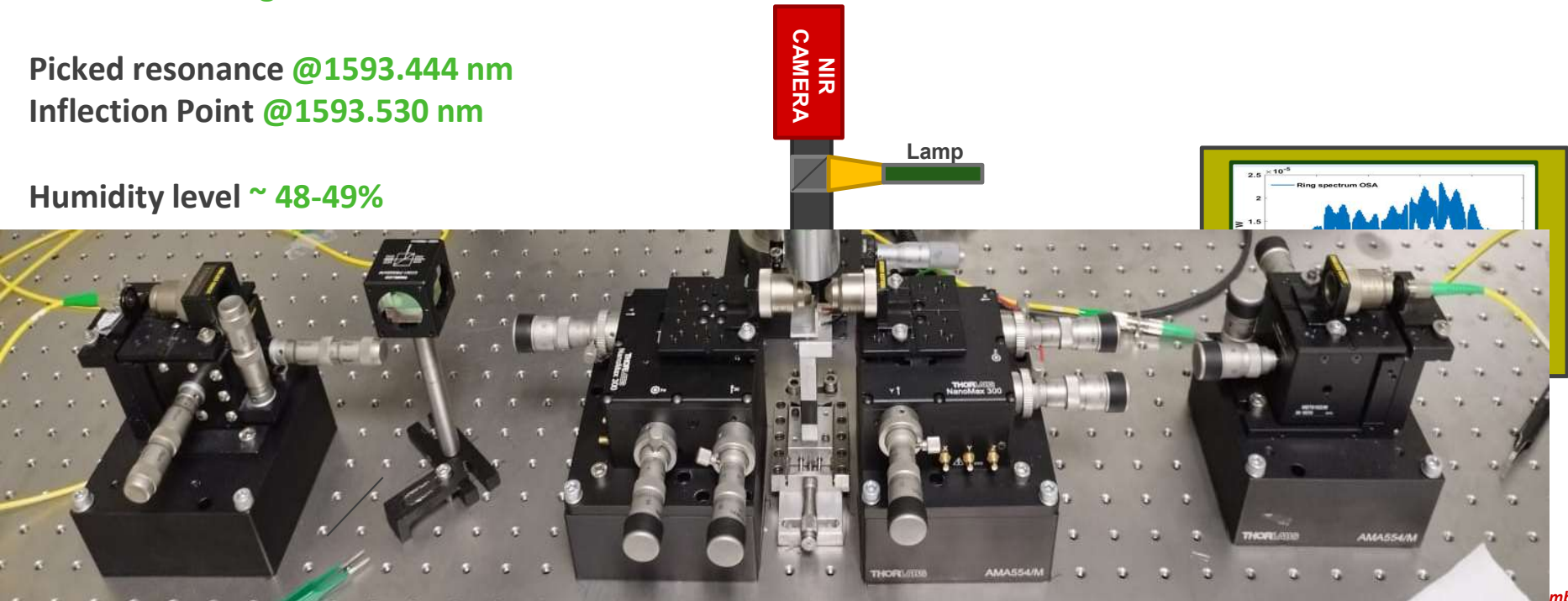
**G400H4R33S** spin-coated with  $\sim 200$  nm PMMA

Sample holder  $T = 20$  °C  
FP effect  $\rightarrow$  fringes

Picked resonance @1593.444 nm  
Inflection Point @1593.530 nm

Humidity level  $\sim 48$ -49%

$$Q = \frac{\nu_0}{FWHM} \sim 8900$$

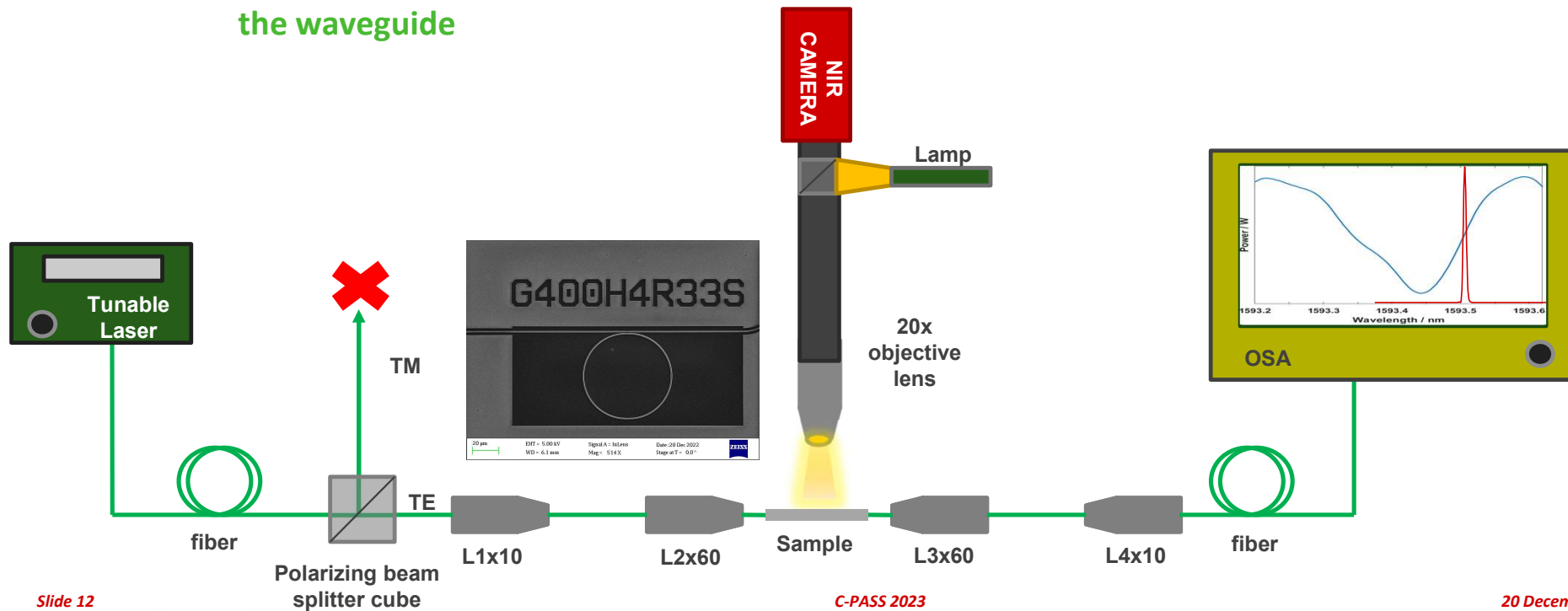


ember 2023



# The experimental setup

End-Fire setup is used to edge-couple the probe laser (TLS – Yenista Optics) tunable laser (1500-1630 nm) onto the waveguide

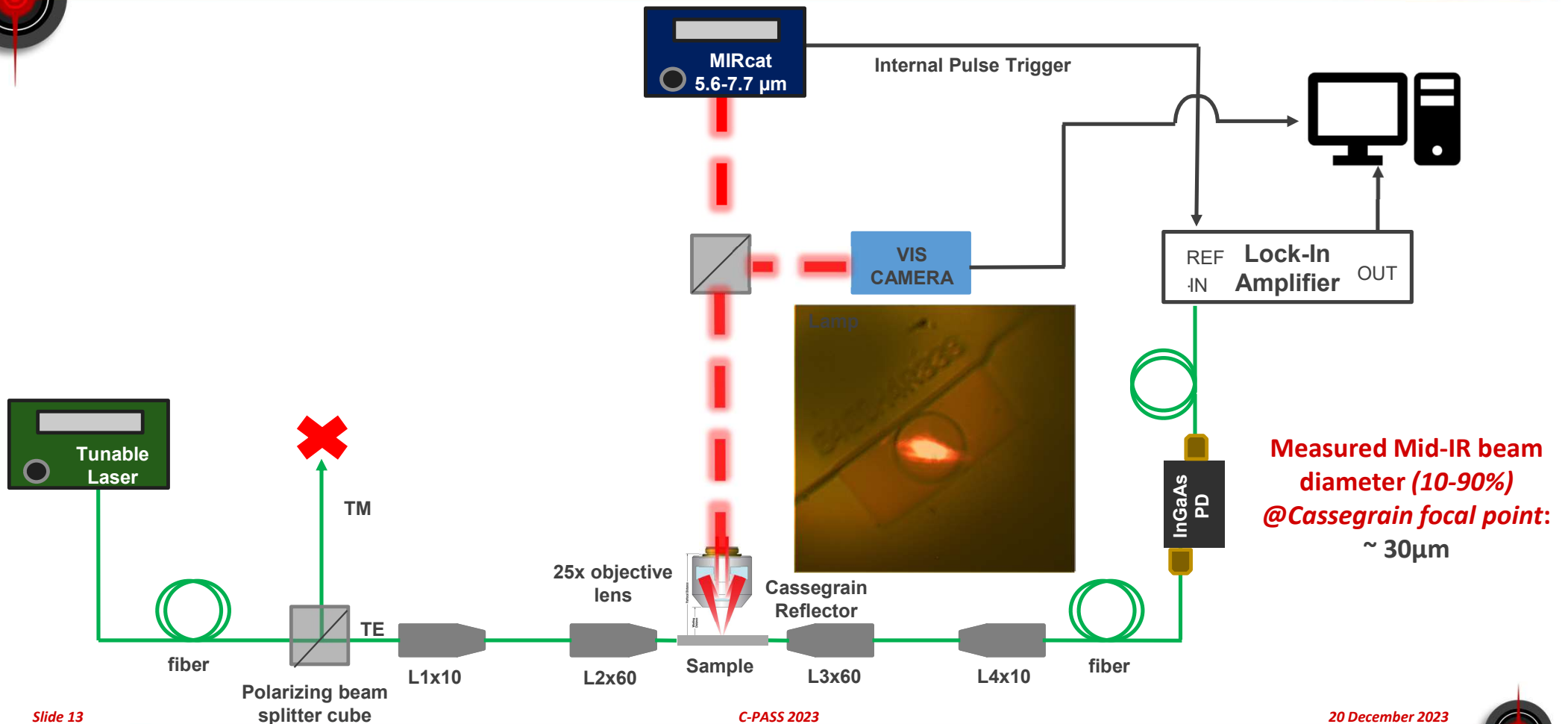


Slide 12

C-PASS 2023

20 December 2023

# The experimental setup



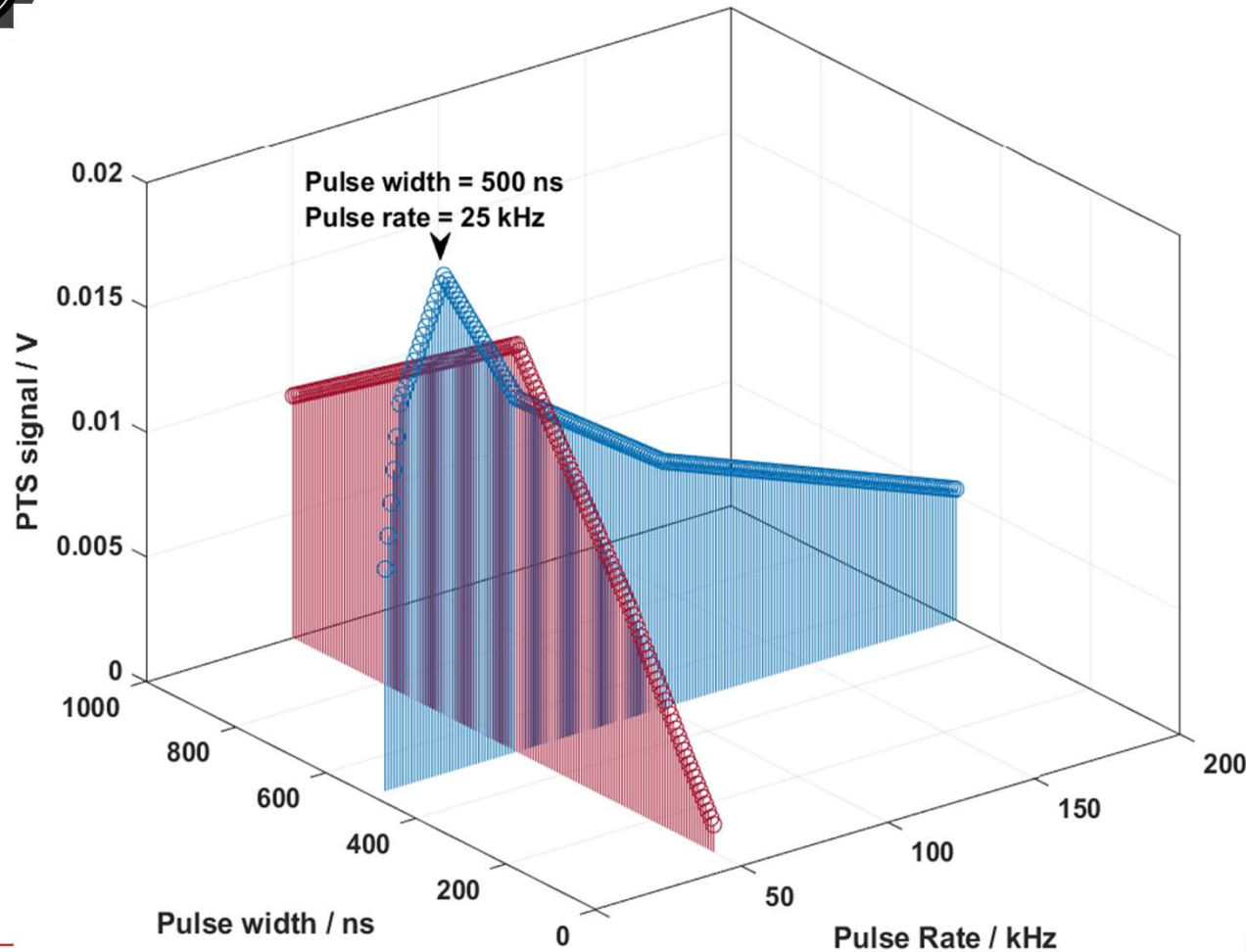
Slide 13

C-PASS 2023

20 December 2023

WWW.OPTAPHI.EU

# Results: optimal operational conditions

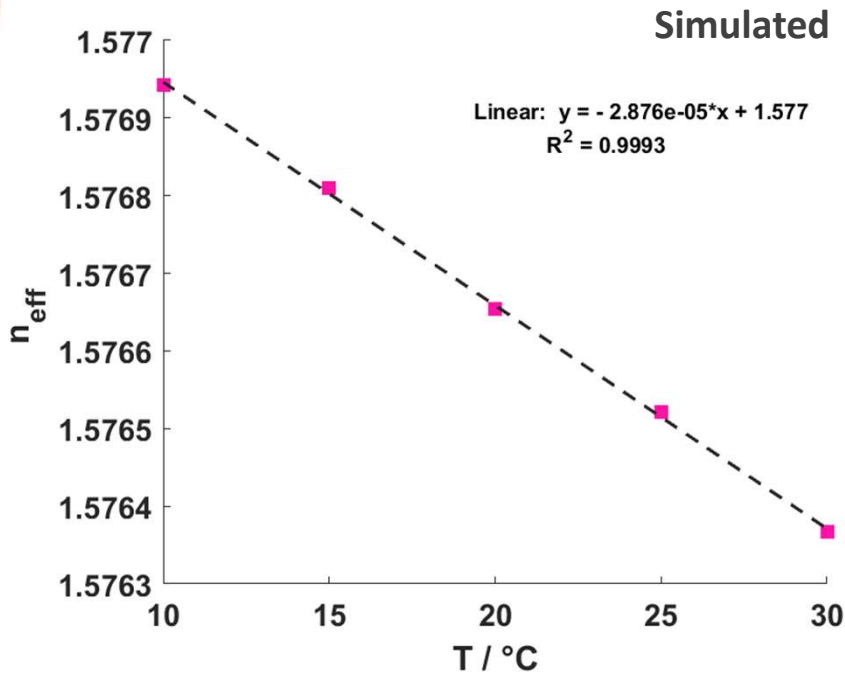


The LIA demodulated signal is maximized using:

- Pulse width= 500 ns
- Pulse rate= 25 kHz
- Duty cycle = 1.25%
- EC-QCL forward sweep scan mode= 5 cm<sup>-1</sup>/step
- LIA time constant  $\tau$ = 100 ms
- EC-QCL operational current= 750 mA

**NO COOLING IS NEEDED FOR THE LASER HEAD IN THE PULSED MODE !**

# The thermo-optical effect of SiN+PMMA, $dn/dT$



**PMMA TOC = -1.3e-4 [RIU/° C]**

$$\Delta T_{SiN + PMMA} \sim +1^\circ C$$



$$\frac{\Delta n_{eff}}{\Delta T} \sim -2.876e-5$$

**Calculated<sup>3</sup>**

$$\frac{\Delta \lambda_{Res}}{\Delta T} = \left( \frac{\Delta n_{eff}}{\Delta T} + n_{eff} \alpha_{TH} \right) \cdot \frac{\lambda_{Res}}{n_{eff}}$$

$$\frac{\Delta \lambda_{Res}}{\Delta T} = -25 \text{ pm}$$

3. Rabus, D. G. Integrated Ring Resonators: The Compendium; Springer series in optical sciences; Springer: Berlin Heidelberg, 2007

Slide 15

C-PASS 2023

20 December 2023

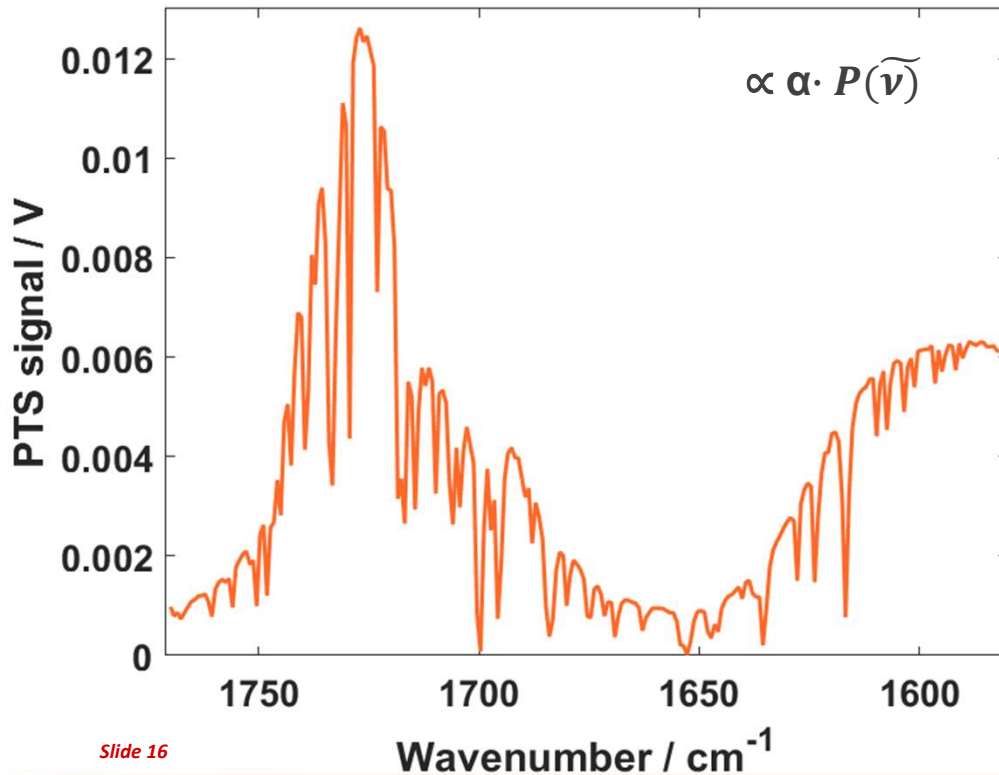
WWW.OPTAPHI.EU



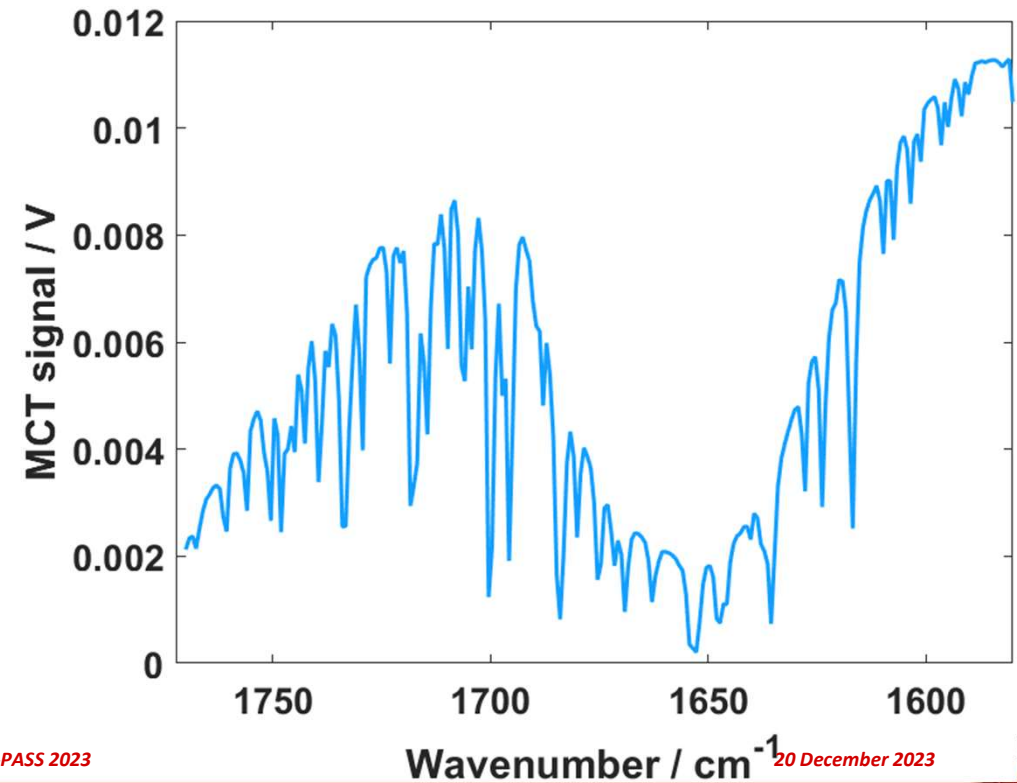


# Results: 200 nm PMMA spectrum

The LIA demodulated PTS signal is acquired by scanning the MIRcat between 1580-1770 wavenumbers on top of the PMMA coated sample



The excitation laser optical power  $P(\bar{\nu})$  has been recorded by means of an MCT detector between 1580-1770 wavenumbers (no interaction with the sample!)



Slide 16

C-PASS 2023

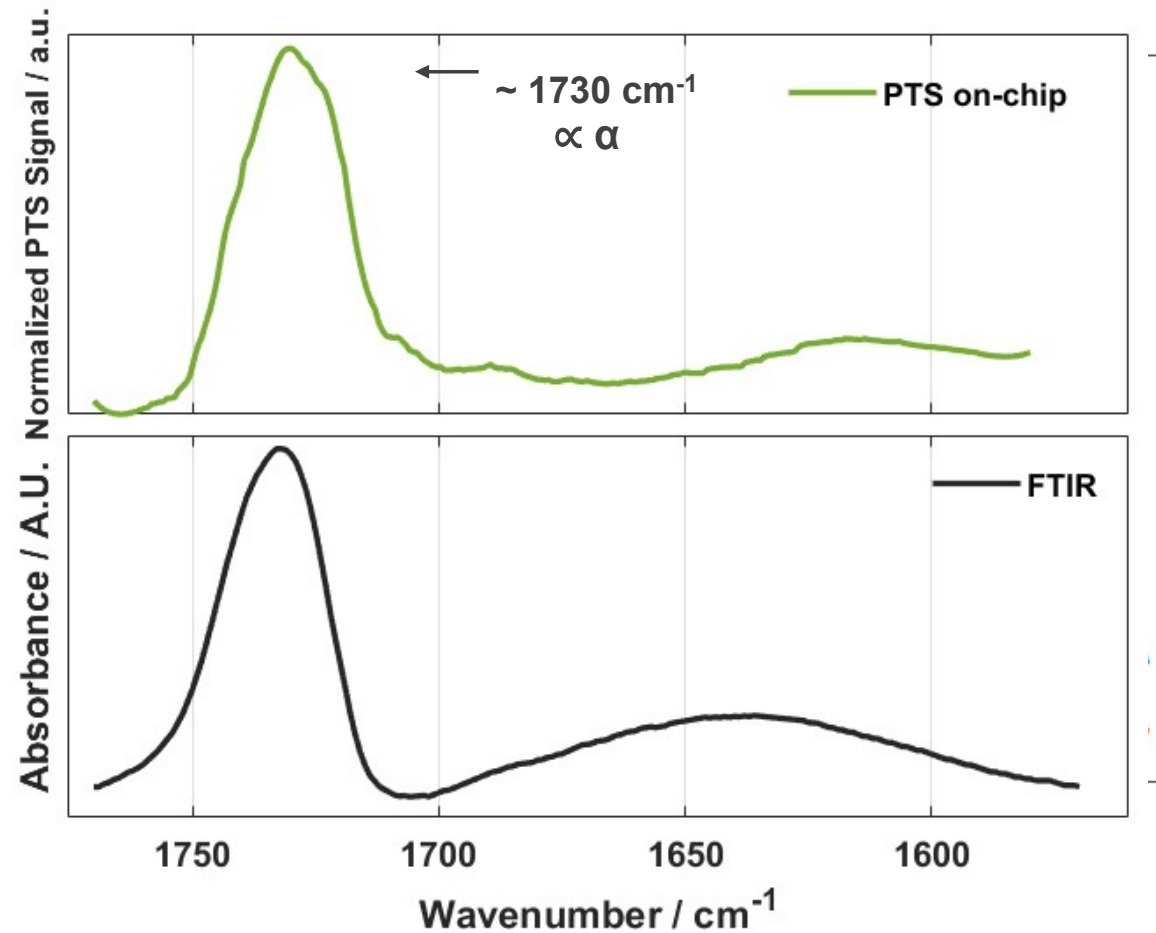
20 December 2023

# Results: 200 nm PMMA spectrum

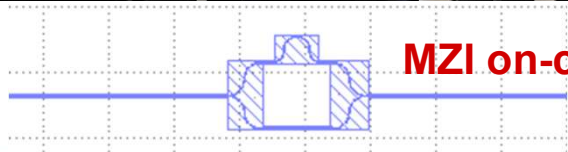
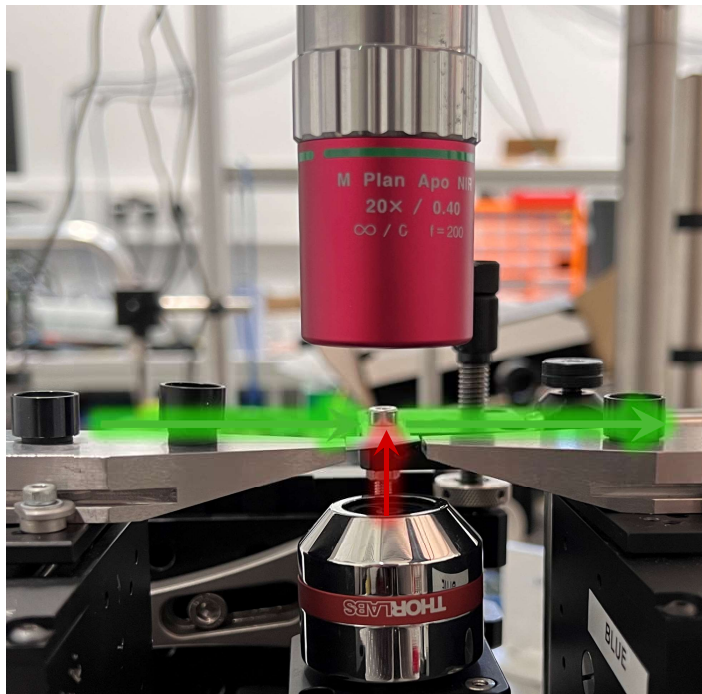
The LIA demodulated signal is normalized by the excitation laser optical power  $P(\nu)$  to retrieve only the analytical information of the target analyte

A Savitzky–Golay filter has been used to remove water vapor contribution

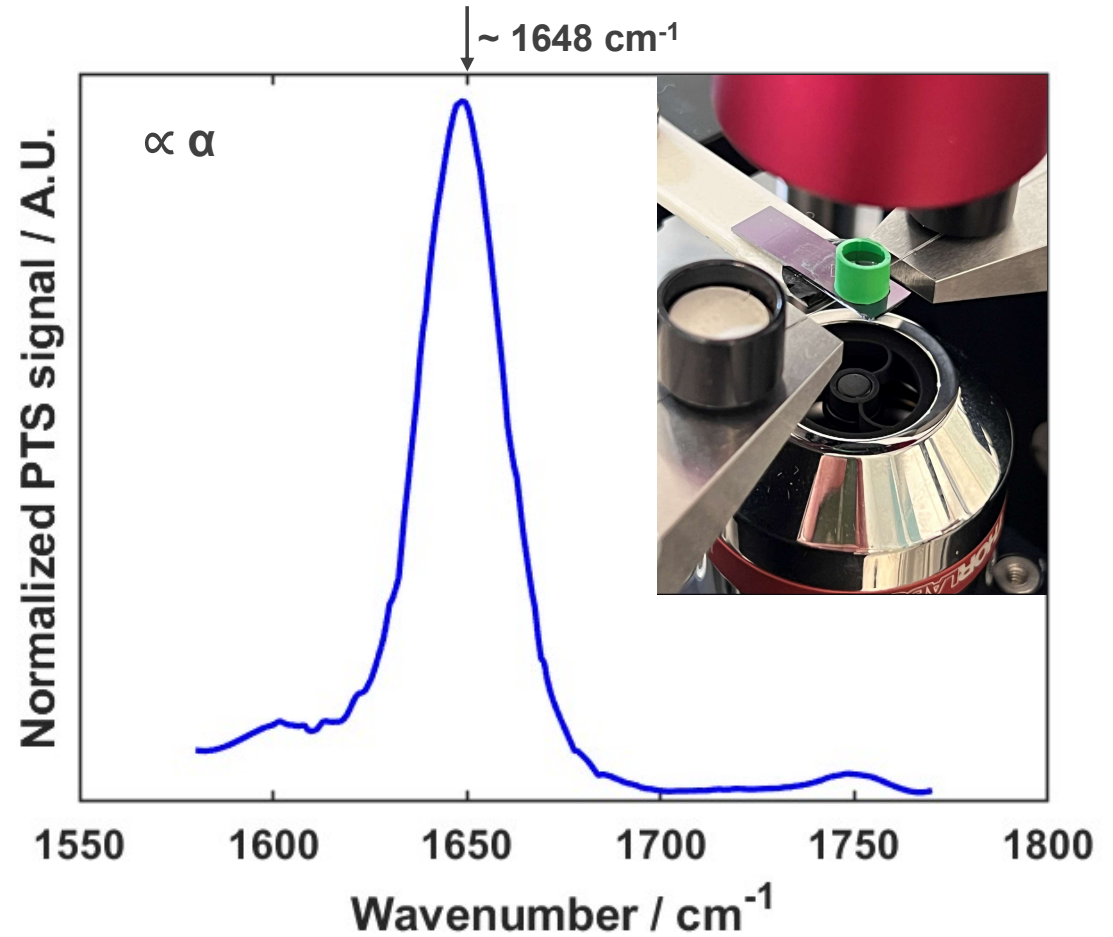
Similar qualitative results have been obtained using a MRR with half the radius



# Current developments & future works



**MZI on-chip**



Slide 18

C-PASS 2023

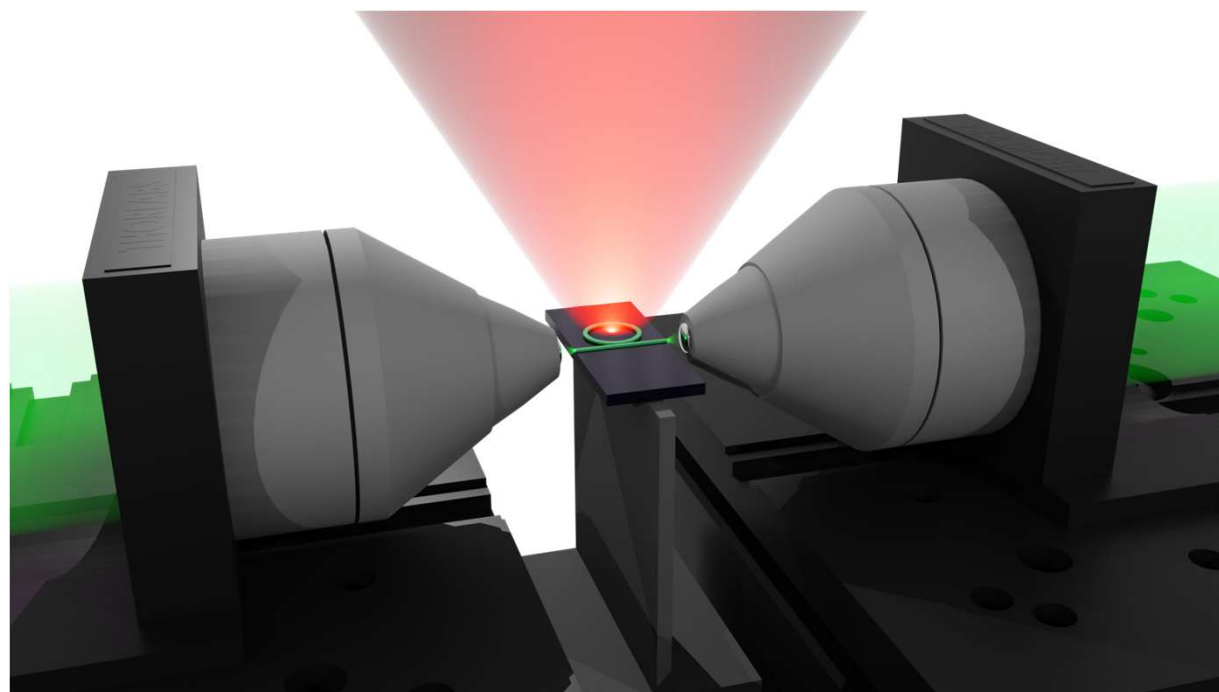
20 December 2023

WWW.OPTAPHI.EU



# Conclusions

- A first demonstration of PTS on-chip using an EC-QCL has been given for targeting PMMA absorption feature
- Qualitative spectra are in excellent agreement with reference method
- Preliminary first demonstration of PTS on-chip for liquid samples has been shown
  - Attractive solution especially for proteins detection where small pathlengths are needed to probe in aqueous solutions



Greetings

**C-PASS**  
Conference on Photonics  
for Advanced Spectroscopy and Sensing




# THANK YOU ALL!



Slide 20

C-PASS 2023

20 December 2023

 OPTAPHI has received funding from the European Union's Horizon 2020 research and innovation programme under the Marie Skłodowska-Curie grant agreement No. 860808



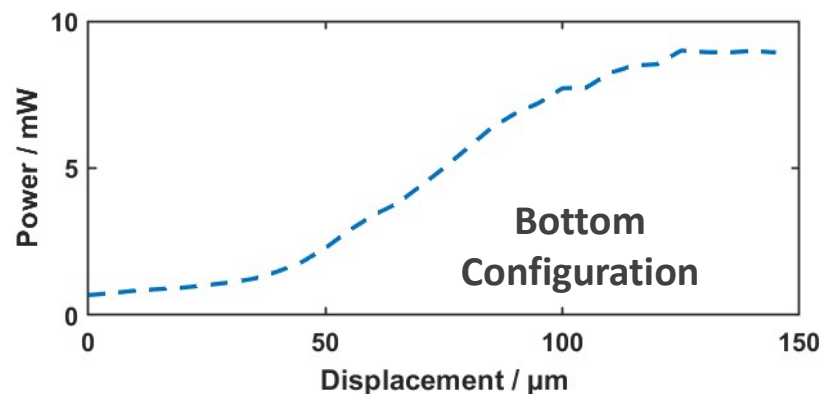
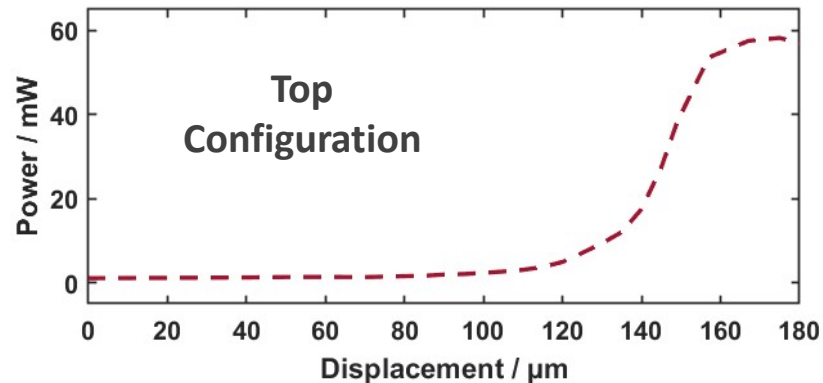
[WWW.OPTAPHI.EU](http://WWW.OPTAPHI.EU)



# Recent results: bottom excitation using a Cassegrain Reflector

## CONS:

- **LESS Mid-IR OPTICAL POWER AVAILABLE**
- **BEAM SPOT SIZE LARGER IN COMPARISON WITH TOP EXCITATION CONFIGURATION**



### Beam Properties

|                    |   |
|--------------------|---|
| Spatial Mode       | TEM <sub>00</sub> (nominal)   |
| Pointing Stability | MIRcat-QT: < 2 mrad (centroid change)<br>MIRcat-1xxx: < 2mrad per 100 cm-1 of tuning (centroid change)  |
| Beam Waist         | < 2.5 mm (1/e <sup>2</sup> intensity radius, typical value, varies with $\lambda$ )<br>30 to 50 cm from output port (typical value, varies with $\lambda$ ) |
| Beam Divergence    | < 4 mrad (full angle, 1/e <sup>2</sup> intensity width, varies with $\lambda$ , measured at with $\lambda = 4 \mu\text{m}$ )                                |
| Linear             | >100:1, vertically polarized, perpendicular to laser base   |

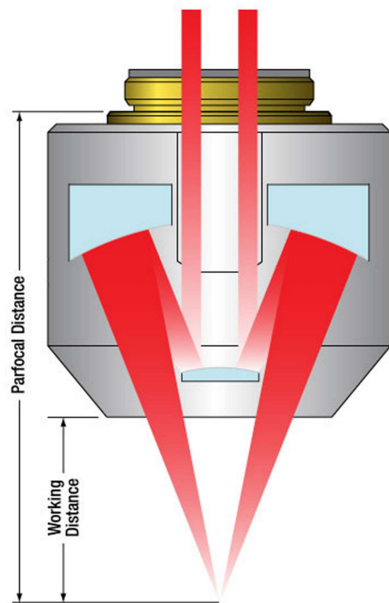
**Mid-IR beam diameter (10-90%)**

**@Cassegrain focal point:**

~ 30  $\mu\text{m}$  (Top excitation)

~ 50  $\mu\text{m}$  (Bottom excitation)





| Item #                                     | LMM15X-P01   | LMM25X-P01        | LMM40X-P01        |
|--|--|-------------------|-------------------|
| Mirror Coating                             | Protected Silver<br>( $R_{avg} > 97\%$ Over 450 nm - 2 $\mu\text{m}$ ;<br>$R_{avg} > 95\%$ Over 2 $\mu\text{m}$ - 20 $\mu\text{m}$ ) |                   |                   |
| Magnification <sup>a</sup>                 | 15X  | 25X               | 40X               |
| Numerical Aperture                         | 0.3  | 0.4               | 0.5               |
| Focal Length                               | 13.3 mm  | 8 mm              | 5.0 mm            |
| Parfocal Distance <sup>b</sup>             | 63.3 mm  | 45.0 mm           | 30.0 mm           |
| Back Focal Length                          | Infinity   | Infinity          | Infinity          |
| Design Tube Lens Focal Length <sup>c</sup> | 200 mm   | 200 mm            | 200 mm            |
| Entrance Pupil Diameter <sup>d</sup>       | 8.0 mm   | 6.4 mm            | 5.1 mm            |
| Working Distance <sup>b</sup>              | 23.8 mm  | 12.5 mm           | 7.8 mm            |
| Field of View                              | 1.2 mm   | 0.7 mm            | 0.5 mm            |
| Resolution <sup>e</sup>                    | 1.1 $\mu\text{m}$  | 0.8 $\mu\text{m}$ | 0.7 $\mu\text{m}$ |
| Obscuration <sup>f</sup>                   | Secondary Mirror Only  | 22%               | 22%               |
|  | Mirror and Spider Vanes  | 26%               | 26%               |
| Transmitted Wavefront Error                | < $\lambda/14$ RMS at 450 nm   |                   |                   |
| Damage Threshold                           | Pulsed 1.0 J/cm <sup>2</sup> (1064 nm, 10 ns, 10 Hz, $\varnothing$ 0.230 mm)   |                   |                   |
| Objective Threading                        | 36 (RMS)   |                   |                   |
| RMS Thread Depth                           | 4.7 mm   | 4.5 mm            | 4.7 mm            |

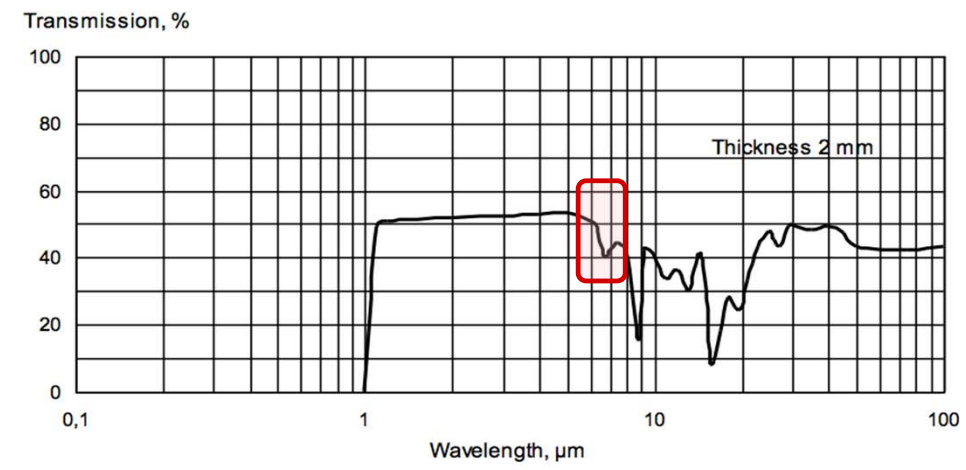
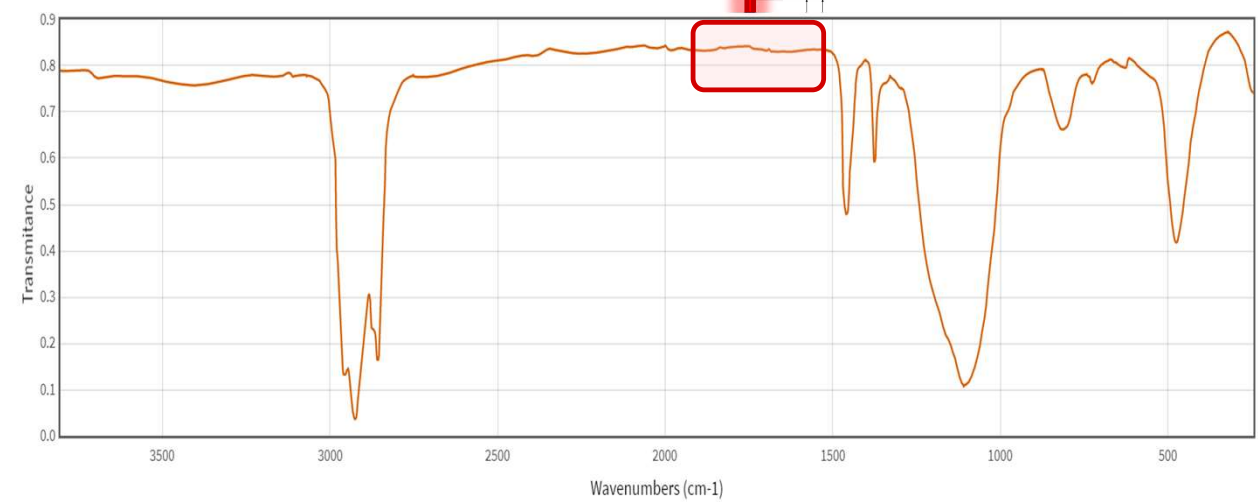
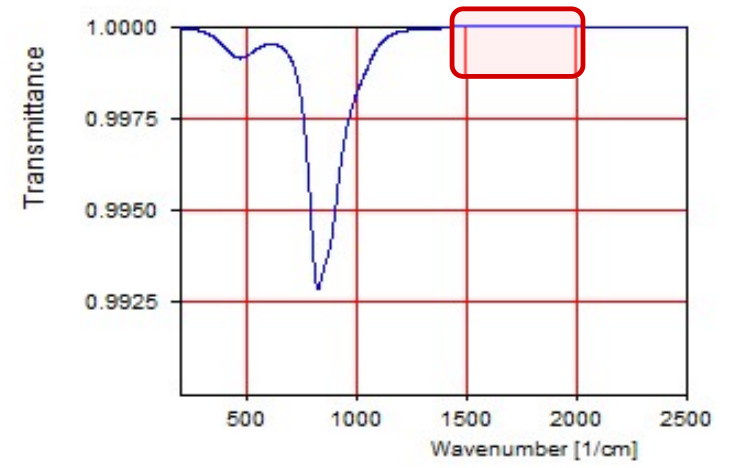
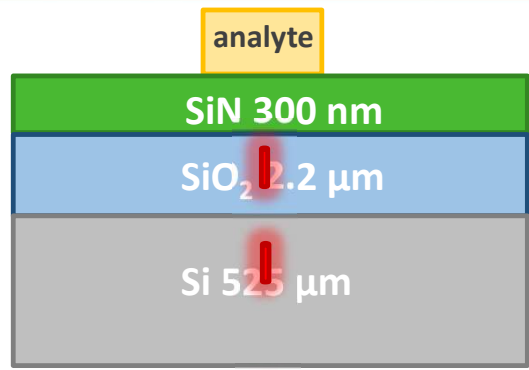
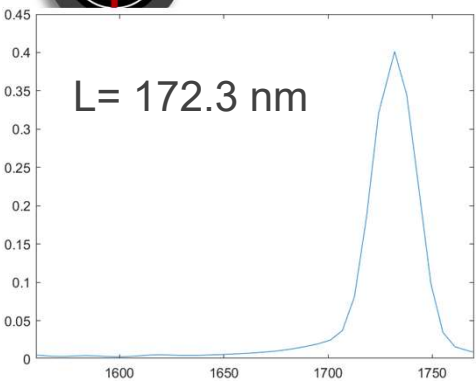


OPTAPHI has received funding from the European Union's Horizon 2020 research and innovation programme under the Marie Skłodowska-Curie grant agreement No. 860808



WWW.OPTAPHI.EU





OPTAPHI has received funding from the European Union's Horizon 2020 research and innovation programme under the Marie Skłodowska-Curie grant agreement No. 860808



WWW.OPTAPHI.EU

